International Review on Computers and Software (I.RE.CO.S.), Vol. 11, N. 3
ISSN 1828-6003 March 2016

Real Time Fatigue-Driver Detection from Electroencephalography Using Emotiv EPOC+

Riyanarto Sarno, Brilian T. Nugraha, M. Nadzeri Munawar

Abstract – *The fatigue driving detection has been developed with many kinds of approaches, such as video using face expressions and Electroencephalography (EEG) that uses the brainwave signals of the driver. This paper proposes a method to implement the driving fatigue detection in real time using Python and Emotiv EPOC+ with 14 channels. The EEG recorded database will extract their features per-30 seconds.*
The prediction process gets the EEG recorded data from the driver doing the driving simulation and trains it using the extracted features data from the database. The results print as Fit and Alert, or Fatigue and Sleepy. The contributions of the authors in this paper are as follows: i) the reduction of the processing time, such as reading input and output files and communicating among different programming languages; ii) the analysis and comparison of the dynamics of prediction results and significant channels from the results of the previous research, and iii) the development of the system from semi real-time to real-time forecasting.

Keywords*: Driver Fatigue Detection, Electroencephalogram (EEG), Find Significant Channels*

Nomenclature

σ_X	Standard deviation on each row (*x*) or per-channel
X_i	EEG data per channel in each row and column
$\bar{X}$	Average EEG data in each row or per-channel
n	Length of EEG data in each row or per-channel
X_k	EEG data in each row or per-channel
e	Euler's number
$-j$	Imaginary symbol
k	The number of each channel
X_{k2i}	EEG even-data per channel
X_{k2i+1}	EEG odd-data per channel
$d(t,u)$	Canberra Distance between data t and u
t_i	EEG data-t per channel and column-i
u_i	EEG data-u per channel and column-i

I. Introduction

Fatigue driving has been found the leading cause of the traffic accidents in the world for years. Fatigue driver detection has been determined by several papers [1]-[4], where the main part used the Electroencephalography (EEG) approach [1]-[3] and the others used the image processing approach [4].

EEG is a method to measure the brainwave by monitoring the brainwave electricity movements. This measurement could be used to identify the fatigue driver by monitoring and processing the brainwave electricity movements. EEG is not the only method to predict the fatigue driver. A research had used the video to classify the fatigue driver state.

The face of the driver will be filmed by a camera with 15 fps video sequences and it will be transformed into YCbSr and HSV spaces from RGB space. The face expressions will be separated, and the eye-blink intervals will be thresholded using K-means clustering. The research gives accuracy results with an average accuracy of 93,18% and the detection rate of 92,71% from 35000 image frames [5].

[6] has used EEG to determine the fatigue driver state using the comparisons between the left prefrontal attention and meditation from EEG with 18 participants (12 males and six females) in noninvasive real-time. The research used the correlation between meditation and attention among concentration state, relaxation state, fatigue state, and sleep state to determine the fatigue driver state. The sensitivity and specificity accuracy results of the research are 63,81% (fatigue drivers) and 90,43% (regular drivers) .

Another research has used EEG to determine fatigue driver state in semi-real-time, the significant channels, and the best features to represent the data using the participant not outliers for the database, and to compare the accuracy results of the statistical analysis with the preprocessing methods (ICA and PCA) [7]. The results showed that using the statistical analysis gives better results than using the preprocessing methods. The research from the statistical analysis method has given accurate results using the KNN classification method with maximum average accuracy 96%, minimum accuracy 90%, maximum accuracy 100%, true positive 45%, true negative 51%, false positive 2%, and false negative 2%; while using the SVM classification method

 DOI: 10.15866/irecos.v11i3.8562

give accuracy results with maximum average accuracy 81%, minimum accuracy 60%, maximum accuracy 90%, true positive 43%, true negative 38%, false positive 4%, and false negative 4%.

In this paper, the researchers modify and develop which has been done [7] from semi-real-time to real-time prediction, increasing the processing time and the accuracy results of the prediction with the training data from the selected participants (participant 2, 4, 10, 11, 16, 17, 18, 21, 22, 23, 24, 26, 27, 28, and 30) using FFT with band wave: theta, alpha, beta, and gamma (TABG).

This paper also analyzes the dynamics prediction results, comparing the significant channels with the outcome of the previous research and the significant channels taken from the dynamics prediction results, determining the best-selected waves to predict the fatigue driver state.

This paper could also be implemented in different fields, such as [8]-[12].

II. Materials and Methods

This chapter describes the materials, the methods, and the comparisons between the previous researches and the methods used in this paper.

II.1. Literature Reviews

The EEG data from the previous research were extracted from the driving simulation done by 30 participants using Emotiv EPOC+ and Logitech G27 game simulator to support the simulation process.

The label data from the driver were taken by raising their finger based on the Karolinska Sleepiness Scale (KSS) [13] modified questionnaire (modified means that the range changed from 1-9 into 1-5) [7] as shown in the Fig. 1.

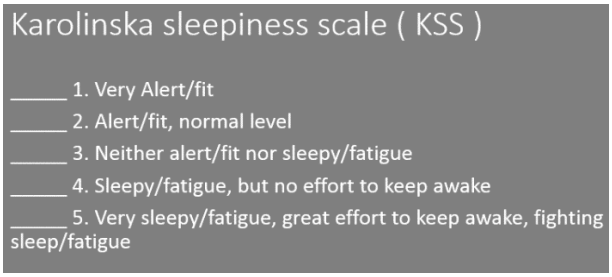

Fig. 1. The KSS modified Questionnaire

The driving simulation duration for each participant is 33 or 60 minutes, for women and men respectively.

The environments of the driving simulation are shown in the Fig. 2. The rules of the driving simulation from the previous research are as follows:

a. Maximum gear allowed to be used is second.
b. Maximum speed is 89 km/h.
c. The allowed transmissions are manual or semi-manual.
d. Both hands should be on the steering wheel.
e. Each participant will be taken their questionnaire record for every 3 minutes.
f. The test durations are 60 minutes for men and 33 minutes for women in total.

The participants should be calm in the driving process, i.e. minimize the body movements, do not vibrate the body, and do not talk during the driving simulation.

The Average method is used to know the domination position values of the data. It could be used to normalize the EEG data that jump unnaturally. The Standard Deviation method is used to know the spreading of the data. It will use the distance between each data with the average data value and square the distance result for each data. The equation of the Standard Deviation method is shown in the Eq. (1):

$$\sigma_X = \sqrt{\frac{\sum_{i=1}^{n}(X_i - \bar{X})^2}{n-1}} \tag{1}$$

A closer standard deviation value to 0 means that the spreading of the data is getting closer. Fast Fourier Transform (FFT) is used to transform the EEG data from time domain to frequency domain. The FFT is a more rapid process of the Discrete Fourier Transform (DFT) using the equation of odd and even data. FFT transforms the DFT equation into the even and odd equation as shown in the Eqs. (2), (3), and (4):

$$X_k = \frac{1}{n}\sum_{i=1}^{n} X_i e^{-j\,2\,\pi\,k\,i\,/n} \tag{2}$$

$$X_k = \frac{1}{\frac{n}{2}}\sum_{k=1}^{\frac{n}{2}} X_{k2i} e^{-j\,2\,\pi\,k\frac{2i}{\left(\frac{n}{2}\right)}} + \\ + \frac{1}{n/2}\sum_{i=1}^{n/2} X_{k2i+1} e^{-j\,2\,\pi\,k\,(2i+1)/\left(\frac{n}{2}\right)} \tag{3}$$

$$X_k = \frac{1}{n/2}\sum_{i=1}^{n/2} X_{\mathrm{k2}i} e^{-j\,2\,\pi\,k\,(2i)/\left(\frac{n}{2}\right)} + \\ + e^{\left(-j\,2\,i\frac{k}{\mathrm{n}}\right)}\frac{1}{n/2}\sum_{i=1}^{n/2} X_{\mathrm{k2}i+1} e^{-j\,2\,\pi\,k\,(i)/\left(\frac{n}{2}\right)} \tag{4}$$

The Canberra Distance method is used to determine the distance between two data, where the range will be more visible with the input data values < 1. The equation of the Canberra Distance method is shown in the Eq. (5):

$$d(t,u) = \sum_{i=1}^{n}\frac{|t_i - u_i|}{|t_i + u_i|} \tag{5}$$

The Cross-validation method is used to predict the estimation accuracy of the methods [14] and to separate the training data and the testing data.

Fig. 2. The driving simulation environments

In the previous research, both the training data and the testing data that will be classified, were extracted from the database, so a separator will be needed for the training data and the testing data which is the main purpose of the use of the cross-validation method.

The K-Nearest Neighbor classification method (KNN) is used to categorize the input data with the training data using Canberra Distance method. The KNN method will measure the relations between the input data with the training data using the distance from the input data and the training data. As a result, the K-nearest training data from the input data will be taken their labels to determine the majorities class of the input data.

The measurement of the fatigue driver uses 14 channels of Emotiv EPOC+ as shown in the Fig. 3.

II.2. Comparisons With The Previous Research

The previous research used Python, Matlab, HTML, and CSS to communicate among each programming language. The features in the research are classification and prediction. The previous research steps using semi-real-time classification were as follows:

a. Feature extraction, where the EEG data trialed features from each participant (for each trial, there were 14 channels, where each channel was composed by the FFT process and four band waves extraction).
b. The features of each wave were taken (the average and the standard deviation values).
c. Semi-real-time prediction, where both the training data and the testing data were extracted from the database that will be determined using the Cross Validation method.
d. The classification methods to determine the prediction result used SVM and KNN classification methods. In this research, the purpose of the classification methods was to determine which classification method was better for classifying the fatigue driver state.
e. The SVM classification method used in the previous research was Linear SVM.
f. The measurement method used in the KNN classification process from the previous research was Canberra Distance.

The architectural design of the previous research is shown in the Fig. 4. In the proposed methods, the programming language to be used is Python, and the EEG data input is extracted from the EEG participant data doing the driving simulation to make a real fatigue driver prediction. The procedure steps used in the proposed methods are as follows:

a. Feature extraction, where the EEG database features from the previous research will be extracted and labeled as training data.
b. Real-time prediction, where the participants do the driving simulation for every 30 seconds and have their EEG data recorded using Emotiv EPOC+, then the recorded EEG data will be extracted per 128x30 or 30 seconds data and with their features (average and standard deviation) extracted, and then the EEG data inputted will be categorized from the training data using KNN classification methods.
c. The specification of the classification methods and the features of each wave employed in the proposed methods are the same as the previous research.

The architectural design of the proposed methods is shown in the Fig. 5. The benefits of the proposed methods are as follows:

a. Reduce the workload of the input or output file reading, and the communication of the different programming language.
b. Increase the processing time.
c. Could be applied directly to the driver, while the previous research could not.

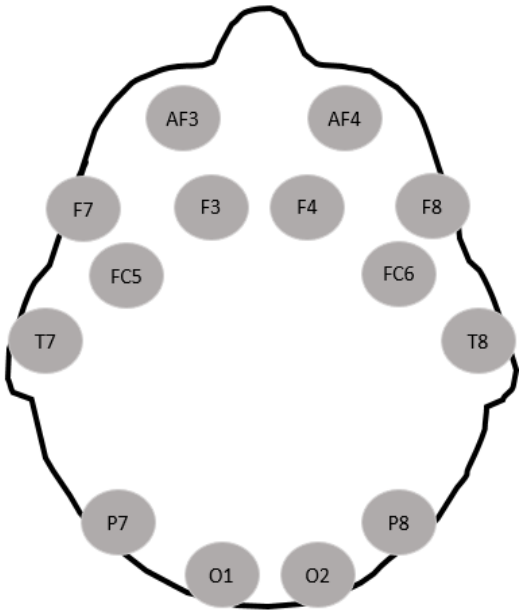

Fig. 3. The 14 channels that will be used to measure the driving fatigue state

II.3. Methods

The propose methods as described in the section *II.2* will do the feature extraction and real-time prediction.

The feature extraction process is shown in the Fig. 6.

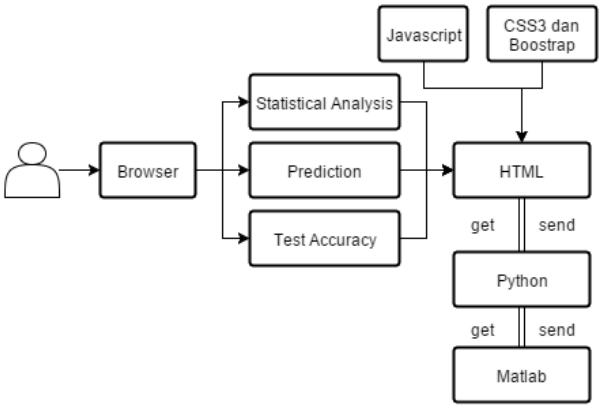

Fig. 4. The architectural design of the previous research

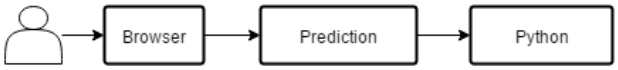

Fig. 5. The architectural design of the proposed methods

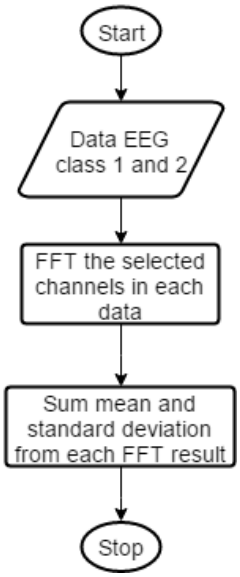

Fig. 6. Feature extraction process to simplify and used as the representative of the EEG data in the classes

The processes of classification and prediction are shown in the Fig. 7. The first assessment processes use the average accuracy results in each part of the EEG trial data from 30 participants to know the accuracy changes of each wave in all channels (from 30 to 180 seconds) per trial and to determine the significant channels and waves. From the first assessment results, the significant channels are determined using the average values of each channel which have been sequenced in the descending order. As a result, the significant channels in the brain location are discovered. Hence, the future works could be simplified to those channels regarding the driver fatigue detection. The second assessment processes use the accuracy results from all participants with the significant channels based on the analysis results of the proposed methods to know the accuracy changes and the prediction results of all participants.

With the results of the second assessment, the proposed methods are compared with the previous research to verify the appropriateness of the used methods. The first assessment will confirm its feasibility to be employed in the real drivers.

The third assessment processes use the accuracy results from all participants with the significant channels and waves from the analysis results of the proposed methods and they compare the previous research and the accuracy results of the proposed methods.

Their results are used to determine the significant waves, and to compare the significant waves of the previous research with such assessment results.

Finally, the fourth assessment processes use the accuracy results from the selected participants of the previous research on the significant channels and waves from the recent works comparing the accuracy results with the previous research using all the participants.

The idea of the fourth assessment results is the same of the third assessment, but it uses only the selected participants as described in the introduction.

The purposes is to measure the actual accuracy results of the proposed method comparing it to the previous research accuracy results and to prove that the features that have been used in the proposed methods give the best results.

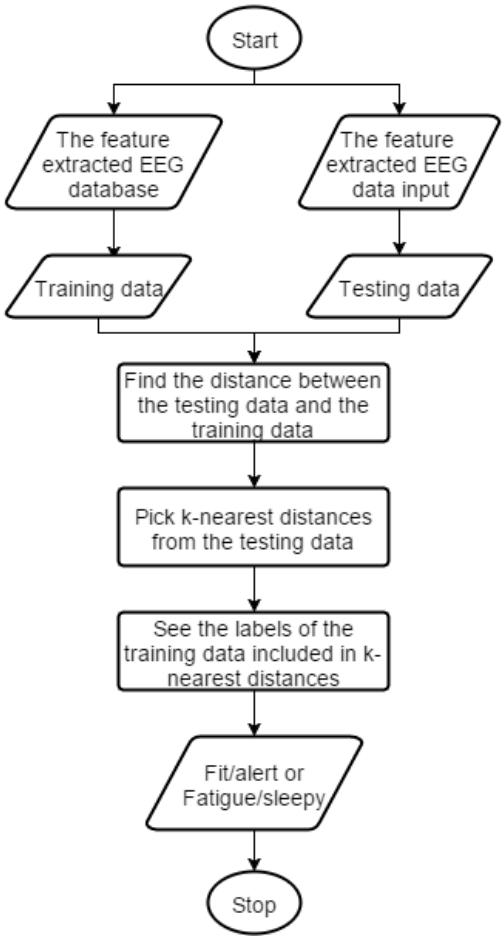

Fig. 7. Real-time classification and prediction process

III. Results

The Emotiv Channels will be named as channel 1 to 14 for comodity. The order of the channels is shown in Table I. The first assessment results from the prediction of 30 participants are shown in Figs. 8, Figs. 9, Fig. 10, Table II, and Table III. As shown in the Figs. 8, the highest wave that gives the best accuracy results is Gamma wave, followed by Beta wave, Alpha wave, and Theta Wave. Figs. 8 show the examples of the average accuracy results from 30 participants with the separated waves (either using theta, alpha, beta, or gamma wave) in one channel. Figs. 9 show the examples of accuracy changes from 30 participants in each channel, i.e. channel 1 to 14 to analyze the dynamics prediction results in each wave for every channel.

The results of the highest wave from 30 participants will be determined in the Fig. 10. Table II shows the accuracy changes in each wave and channel from 30 participants with C as Channel and W as Wave that will be used to predict the participant recorded EEG data from driving simulation. Part 1 to 6 are from the average of trials, where each trial consists of 6 parts, and at this table, the average of all trials in each participant will be taken. In Table III, the waves in each channel from the Table II will be calculated their average, and sorted in the descending order to determine the significant channels based on the accuracy changes using each wave in all channels and all participants. Table III shows the significant channels based on the accuracy changes that have been analyzed from each wave in all participants.

The seven highest significant channels marked by gray colors on Table III are as follows: channel 2, channel 9, channel 11, channel 14, channel 3, channel 6, and channel 8. The average accuracy results from each wave are shown in Fig. 10. From the analysis results that have been shown in Fig. 10, the gamma wave shows as the highest average accuracy results in all participants.

The second assessment results using the significant channels taken from the analysis results of the proposed methods are shown in Table IV with P as the participants and Avg as the average of all Parts in each participant.

Based on Table IV, the participants with high accuracy results (marked by gray color) are the ones with the average accuracy ≥ 60%.

TABLE I
CHANNELS USED IN EMOTIV EPOC+

Channel	The Name of The Channel
1	AF3
2	F7
3	F3
4	FC5
5	T7
6	P7
7	O1
8	O2
9	P8
10	T8
11	FC6
12	F4
13	F8
14	AF4

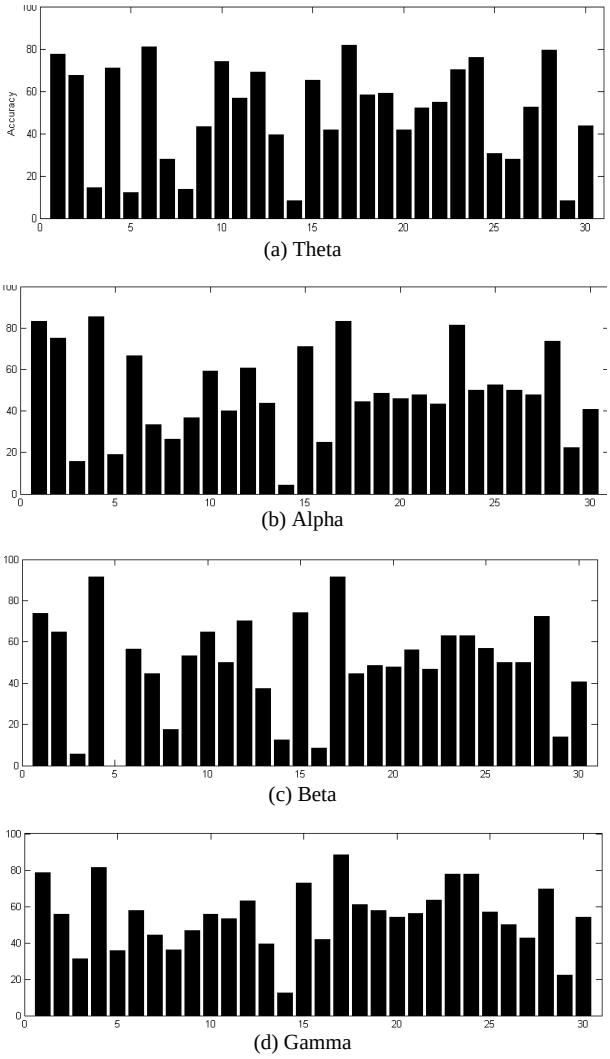

(a) Theta

(b) Alpha

(c) Beta

(d) Gamma

Figs. 8. The examples of the average accuracies from 30 participants using each wave: (a) theta, (b) alpha, (c) beta, and (d) gamma

The third assessment processes compare the accuracy results from the predictions of 30 participants using the significant channels and waves acquired from the proposed methods with the selected channels and all the waves taken from the previous research.

The comparisons of the average accuracy results from all participants are shown in Figs. 11 where all the waves use Theta, Alpha, Beta, and Gamma.

Based on the mean accuracy results in Figs. 11, the highest accuracy of each part is using beta and gamma waves. The detail of the highest accuracy results in each part is shown in Table V.

The fourth assessment processes as in the Figs. 12 are comparing the average accuracy results in each part using the significant channels and the selected waves from the analysis results of the previous research from the selected participants. Based on the comparisons in the Figs. 12, the average accuracy results in Part 6 with all kinds of the selected waves give better accuracy results than the previous research. In Fig. 12(d), the average accuracy results of Part 5 is better than the accuracy result of the previous research.

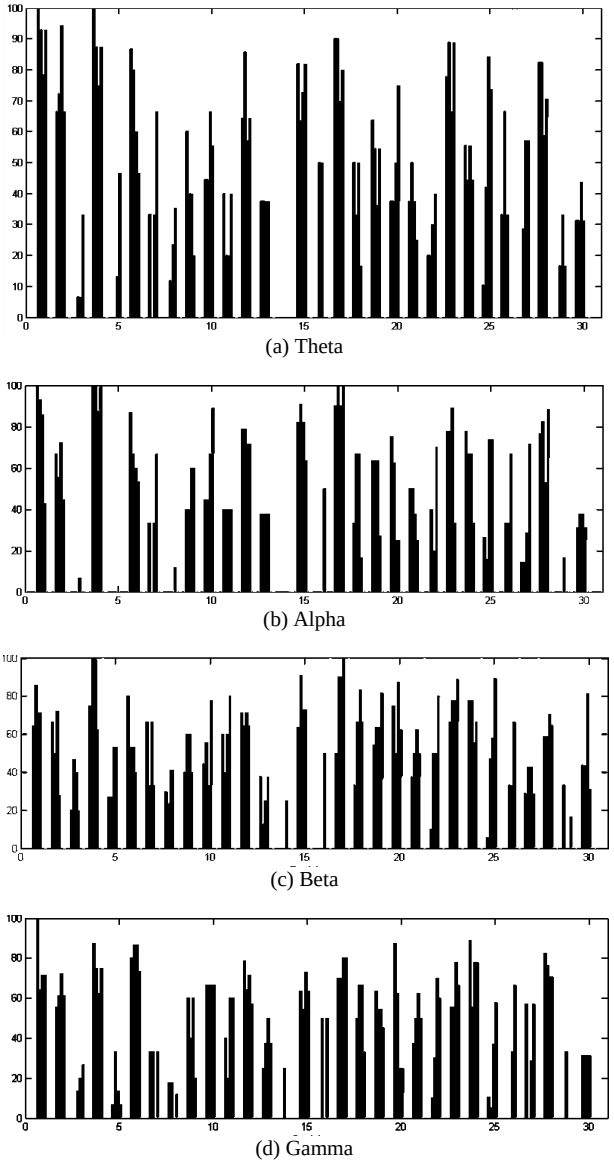

(a) Theta

(b) Alpha

(c) Beta

(d) Gamma

Figs. 9. Examples of accuracy changes using one channel in part 1 to 6 from 30 participants in each wave: (a) theta, (b) alpha, (c) beta and (d) gamma

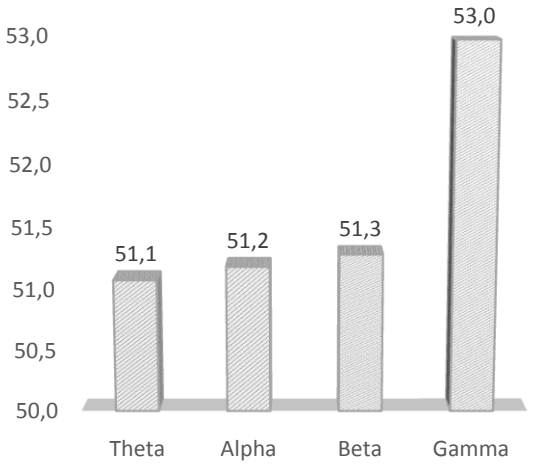

Fig. 10. The mean accuracies result from each wave with gamma wave as the highest wave

TABLE II
ACCURACY RESULTS FROM EACH WAVE IN ALL CHANNELS

C	W	Part 1	Part 2	Part 3	Part 4	Part 5	Part 6	Avg
1	T	45.3	44.5	47.4	47.9	50.3	64.5	50.0
	A	43.5	46.0	47.9	48.3	57.6	52.2	49.2
	B	44.2	45.2	46.8	46.4	53.1	58.5	49.0
	G	44.0	49.8	55.9	56.4	56.3	65.2	54.6
2	T	46.8	47.1	48.6	43.4	53.9	66.6	51.1
	A	45.8	49.9	50.1	53.1	53.4	63.3	52.6
	B	48.6	54.7	52.8	53.5	53.3	61.0	54.0
	G	51.7	52.2	53.2	47.3	52.4	69.0	54.3
3	T	46.9	48.2	45.4	56.1	51.9	68.2	52.8
	A	44.5	53.6	45.6	51.4	53.7	54.5	50.5
	B	44.9	57.4	53.5	49.1	53.4	65.3	54.0
	G	49.0	46.9	52.3	51.2	43.6	63.0	51.0
4	T	45.4	50.0	47.6	47.5	46.7	63.6	50.1
	A	52.8	47.9	51.0	49.5	57.5	54.2	52.1
	B	47.4	52.1	54.0	45.7	51.9	62.7	52.3
	G	47.6	49.3	45.3	51.8	50.2	64.7	51.5
5	T	38.6	47.6	50.0	47.8	48.5	63.3	49.3
	A	43.6	42.2	43.1	49.1	58.9	64.8	50.3
	B	45.8	50.7	55.1	49.7	48.9	56.8	51.2
	G	45.3	43.4	44.2	50.2	50.2	63.9	49.5
6	T	46.2	45.5	53.9	55.1	51.9	65.4	53.0
	A	46.9	43.4	43.1	52.7	53.6	68.7	51.4
	B	48.8	45.8	46.4	42.5	51.7	60.2	49.2
	G	51.6	49.9	54.8	47.3	50.7	67.8	53.7
7	T	46.4	45.9	46.0	49.7	46.9	57.7	48.8
	A	48.2	51.7	48.3	42.2	49.1	58.1	49.6
	B	50.1	56.0	45.5	47.6	48.2	62.7	51.7
	G	51.6	50.2	52.4	56.4	52.3	65.0	54.6
8	T	47.9	48.9	46.7	51.0	56.4	65.5	52.7
	A	54.4	49.8	40.5	44.7	52.6	62.9	50.8
	B	47.6	43.1	47.1	46.1	51.8	62.8	49.8
	G	54.1	49.9	42.6	49.0	55.8	69.5	53.5
9	T	46.2	48.1	49.6	46.6	54.5	63.8	51.5
	A	49.3	45.3	47.4	54.5	53.6	65.7	52.6
	B	49.5	42.2	50.8	47.8	55.0	62.6	51.3
	G	51.6	50.5	47.9	55.7	56.7	68.5	55.1
10	T	44.7	45.2	50.3	51.8	51.3	63.0	51.0
	A	46.7	47.4	43.4	49.8	47.2	63.3	49.6
	B	43.3	45.0	52.2	51.7	49.0	58.8	50.0
	G	43.2	58.1	51.6	44.4	52.8	67.5	52.9
11	T	41.7	51.2	48.6	51.5	52.7	68.0	52.3
	A	47.4	49.8	42.3	54.7	51.9	62.3	51.4
	B	45.7	45.9	52.0	52.2	51.3	61.4	51.4
	G	48.0	54.2	52.3	56.5	55.8	63.3	55.0
12	T	44.9	45.0	49.5	50.3	53.2	59.8	50.5
	A	43.9	46.7	51.2	44.6	57.0	61.2	50.8
	B	44.4	52.6	50.1	53.7	47.7	61.2	51.6
	G	46.3	46.2	48.7	49.8	56.6	67.7	52.5
13	T	41.9	48.4	44.6	48.1	51.3	67.8	50.4
	A	44.2	52.5	51.9	51.1	55.7	65.0	53.4
	B	43.3	42.6	46.1	50.3	51.4	57.1	48.5
	G	43.1	47.3	51.3	45.5	52.5	64.6	50.7
14	T	43.8	56.1	44.7	52.7	49.4	62.8	51.6
	A	46.4	51.1	48.9	47.6	56.2	62.2	52.1
	B	43.9	52.6	58.0	54.0	52.7	61.9	53.8
	G	46.3	50.8	55.4	46.6	50.2	65.0	61.1

TABLE III
SIGNIFICANT CHANNELS BASED ON THE ACCURACY CHANGES FROM ALL WAVES IN ALL CHANNELS

Channel	Average Per Channel	Channel	Average Per Channel
2	53.0	7	51.2
9	52.6	10	50.9
11	52.5	13	50.7
14	52.5	1	50.7
3	52.1	5	50.1
6	51.8		
8	51.7		
4	51.5		
12	51.4		

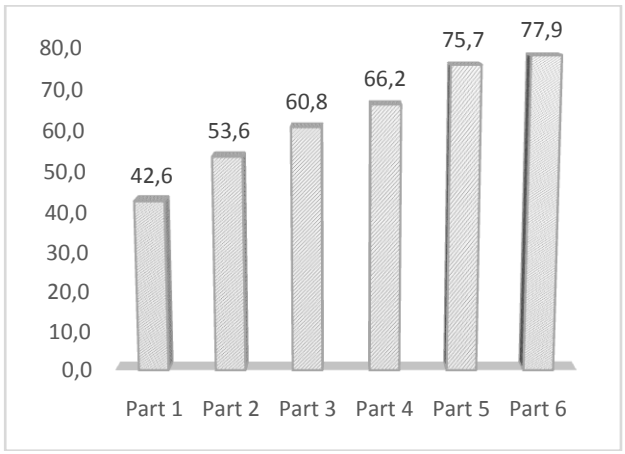

(a) all waves

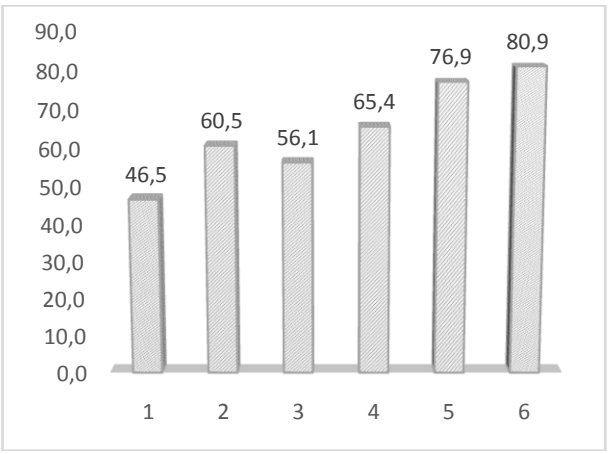

(c) alpha,beta, and gamma waves

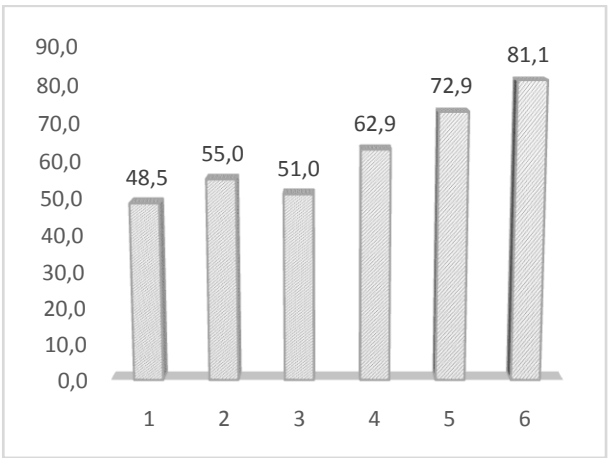

(b) beta and gamma waves

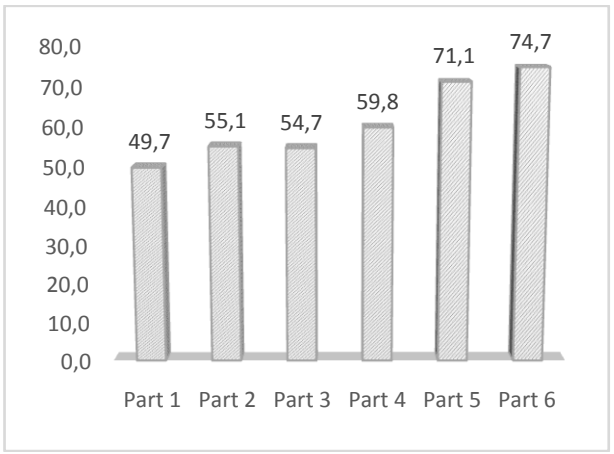

(d) gamma wave

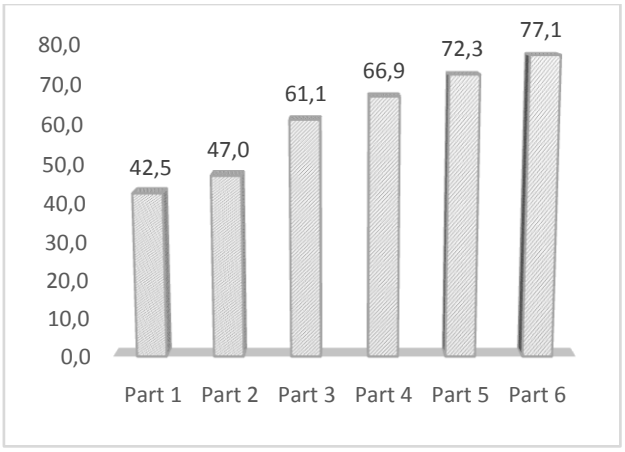

(e) previous research

Figs. 11. The average accuracy results from significant channels and waves with the previous research using: (a) all waves; (b) beta and gamma waves; (c) alpha, beta, and gamma waves; (d) gamma wave and (e) the method of the previous research using all waves

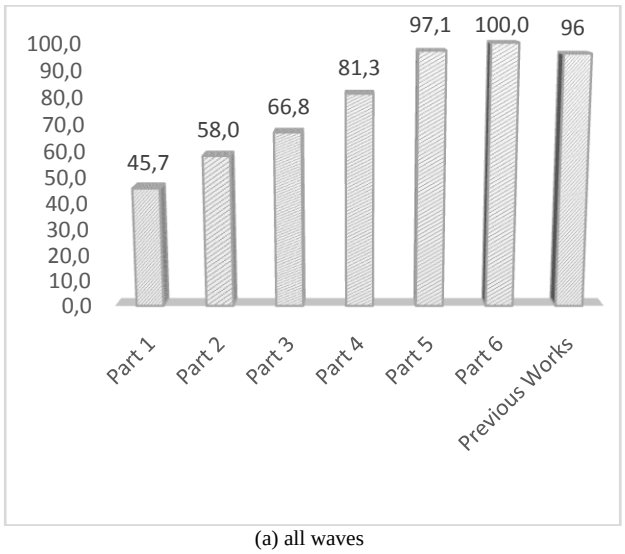

(a) all waves

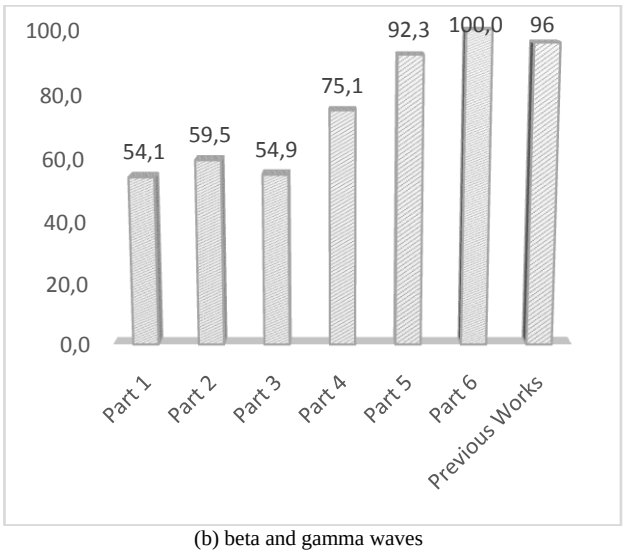

(b) beta and gamma waves

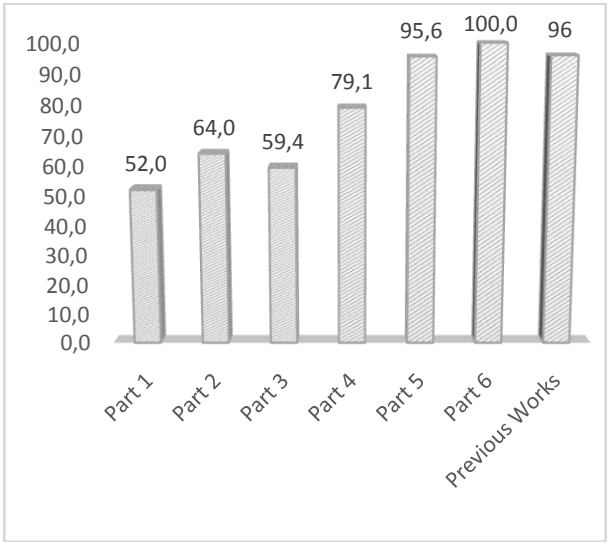

(c) alpha,beta, and gamma waves

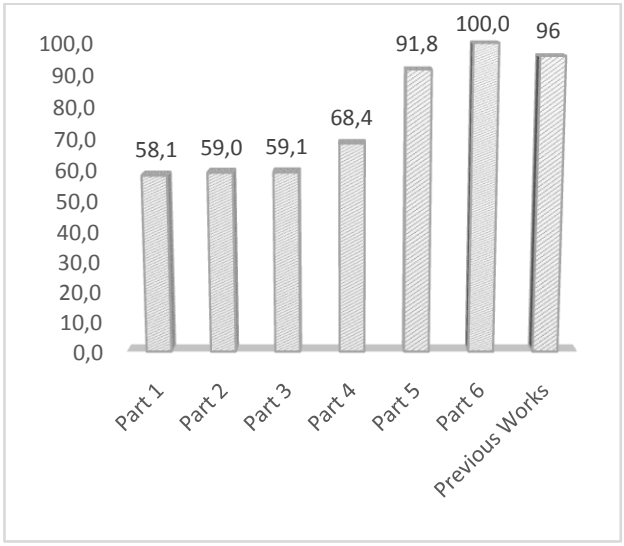

(d) gamma wave

Figs. 12. The comparisons of the average accuracy results in each part using the significant channels, the selected waves, and the selected participants with the previous research using: (a) all waves; (b) beta and gamma waves; (c) alpha, beta, and gamma waves; and (d) gamma wave

IV. Discussions

The significant channels based on the accuracy changes on Table III in descending are channel 2, 9, 11, 14, 3, 6, 8, 4, 12, 7, 10, 13, 1, and 5. The seven highest significant channels are discovered in the prefrontal and occipital cortices. The Prefrontal Cortex is a front part of the human brain used for information processing, decision making, and cognitive control [15]-[16], these brain functions affect the driving behavior of the humans.

The Occipital Cortex is a rear part of the human brain used for visual processing: object recognition, color recognition, motion perception, depth perception, and spatial pattern [17]-[19], these brain functions affect the recognition in the driving environments of the humans.

Based on the two parts of the brain functions with the significant channels from the proposed methods, the channels are declared as suitable for the fatigue driver detection. The significant channel positions and the brain function locations are shown in the Fig. 13 and Fig. 14.

The high accuracy results using the proposed methods are as follows: participant 1, participant 2, participant 4, participant 7, participant 9, participant 10, participant 11, participant 14, participant 16, participant 17, participant 18, participant 19, participant 21, participant 22, participant 23, participant 24, participant 26, participant 27, participant 28, and participant 30.

The reason is the condition of the participants: the participants with high accuracy results were calm or following their experiment of driving simulations conditions. Hence, the other participants with lower accuracy results were not calm or ignoring some of the driving simulation conditions. The comparison results in the Figs. 11 and Figs. 12 show that the proposed methods give better accuracy results using the beta and gamma waves (based on part 6). However, using all the waves for the participants who follow the driving simulation rules give the best accuracy results.

TABLE IV
DETAIL OF THE AVERAGE ACCURACY FOR EACH PART USING THE SIGNIFICANT CHANNELS FROM 30 PARTICIPANTS

P	Part 1	Part 2	Part 3	Part 4	Part 5	Part 6	Avg
1	35.7	78.6	85.7	85.7	85.7	64.3	72.6
2	33.3	38.9	83.3	100.0	100.0	100.0	75.9
3	26.7	66.7	60.0	53.3	46.7	66.7	53.3
4	100.0	100.0	87.5	87.5	100.0	100.0	95.8
5	13.3	66.7	60.0	66.7	53.3	66.7	54.4
6	26.7	6.7	46.7	60.0	40.0	33.3	35.6
7	33.3	66.7	66.7	66.7	66.7	66.7	61.1
8	11.8	41.2	58.8	47.1	41.2	35.3	39.2
9	60.0	60.0	80.0	40.0	60.0	60.0	60.0
10	44.4	77.8	88.9	88.9	100.0	100.0	83.3
11	80.0	40.0	20.0	60.0	100.0	100.0	66.7
12	78.6	57.1	50.0	35.7	35.7	42.9	50.0
13	12.5	37.5	62.5	50.0	50.0	50.0	43.8
14	0.0	50.0	75.0	100.0	100.0	100.0	70.8
15	63.6	45.5	36.4	27.3	27.3	45.5	40.9
16	0.0	100.0	100.0	50.0	100.0	100.0	75.0
17	90.0	100.0	90.0	100.0	100.0	100.0	96.7
18	66.7	66.7	66.7	83.3	83.3	100.0	77.8
19	27.3	90.9	63.6	63.6	63.6	72.7	63.6
20	62.5	37.5	25.0	37.5	75.0	50.0	47.9
21	37.5	62.5	37.5	87.5	100.0	100.0	70.8
22	30.0	30.0	50.0	90.0	90.0	100.0	65.0
23	55.6	44.4	77.8	88.9	88.9	100.0	75.9
24	33.3	55.6	88.9	77.8	100.0	100.0	75.9
25	57.9	15.8	0.0	0.0	52.6	84.2	35.1
26	0.0	0.0	33.3	66.7	100.0	100.0	50.0
27	28.6	57.1	100.0	100.0	100.0	100.0	81.0
28	29.4	52.9	41.2	76.5	100.0	100.0	66.7
29	83.3	16.7	50.0	33.3	16.7	0.0	33.3
30	35.7	78.6	85.7	85.7	85.7	64.3	72.6

TABLE V
THE HIGHEST AVERAGE ACCURACY RESULTS IN EACH PART

Part	The Highest Average Accuracy Result
1	14 (d)
2	14 (c)
3	14 (e)
4	14 (e)
5	14 (c)
5	14 (c)
6	14 (b)

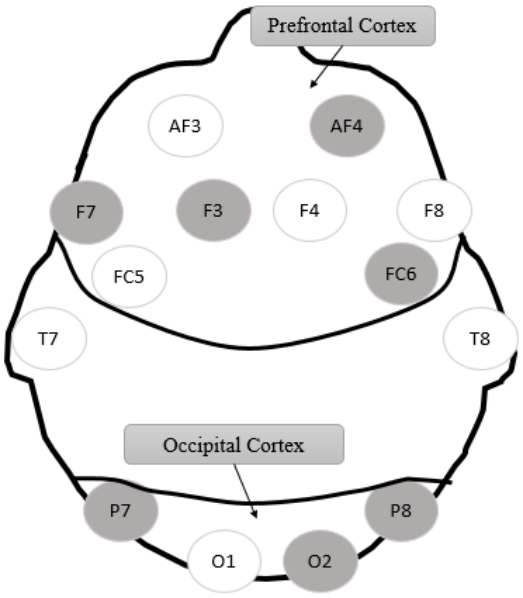

Fig. 13. The seven highest significant channels added with the locations of the brain shown from the above

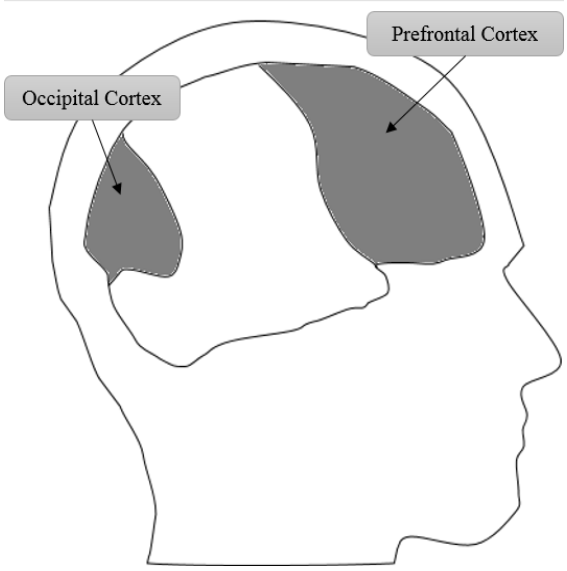

Fig. 14. The locations of the brain from the side

Based on the results and the previous research from the Figs. 11 and Figs. 12, the fatigue driver detection for the selected participants using all the waves is the best option for the behavior of the selected participants.

V. Conclusion

The proposed methods can do the prediction of driving simulation using EEG data with Emotiv EPOC+ in real time with the following details:

a. The significant channels are discovered in the prefrontal and occipital cortices.
b. Using all the waves is the best option for detecting the fatigue driver to the driver who drives calmly.
c. The proposed methods give high accuracy results on the participants who follow the driving rules in the driving simulation.

The future research will carry out fatigue detection based on real-time measurement of actual drivers.

Acknowledgements

Authors would like to thank the Institut Teknologi Sepuluh Nopember and the Ministry of Research, Technology and Higher Education of Indonesia for supporting the research.

References

[1] F. Wang, J. Lin, W. Wang and H. Wang, EEG-Based Mental Fatigue Assessment During Driving by Using Sample Entropy and Rhythm Energy, (2015) *Cyber Technology in Automation, Control and Intelligent Systems*, pp. 1906 - 1911. http://dx.doi.org/10.1109/CYBER.2015.7288238

[2] M. A. Li, An EEG-Based Method For Detecting Drowsy Driving State, *Fuzzy Systems and Knowledge Discovery (FSKD)*, 2010, pp. 2164 - 2167. http://dx.doi.org/ 10.1109/FSKD.2010.5569757

[3] B. C. Chang, J. E. Lim, H. J. Kim and B. H. Seo, A Study of Classification of The Level of Sleepiness For The Drowsy Driving Prevention, (2007) *SICE*, pp. 3084 - 3089.

http://dx.doi.org/ 10.1109/SICE.2007.4421521.
[4] R. Ahmed, K. Emon and M. Hossain, Robust Driver Fatigue Recognition Using Image Processing, (2014) *Informatics, Electronics & Vision (ICIEV)*, pp. 1-6. http://dx.doi.org/10.1109/ICIEV.2014.6850713.
[5] K. Rezaee, H. Sabzevari, S. Alavi, M. Madanian, M. Rasegh Ghezelbash, H. Khavari and J. Haddadnia, Real-time Intelligent Alarm System of Driver Fatigue Based On Video Sequences, (2013) *Robotics and Mechatronics (ICRoM)*, pp. 378-383. http://dx.doi.org/10.1109/ICRoM.2013.6510137
[6] J. He, D. Liu, Z. Wan and C. Hu, A Noninvasive Real-Time Driving Fatigue Detection Technology Based On Left Prefrontal Attention and Meditation EEG, (2014) *Multisensor Fusion and Information Integration for Intelligent Systems (MFI)*, pp. 1-6. http://dx.doi.org/10.1109/MFI.2014.6997673.
[7] B. T. Nugraha, R. Sarno, D. A. Asfani, T. Igasaki and M. N. Munawar, Classification of Driving Fatigue State Based On EEG Using Emotiv EPOC+, (2016) *Journal of Theoretical and Applied Information Technology*, 86(3), pp. 1-14.
[8] R. Sarno, B. A. Sanjoyo, I. Mukhlash and H. M. Astuti, Petri Net Model of ERP Business Process Variation for Small and Medium Enterprises, (2013) *Journal of Theoretical and Applied Information Technology*, 51(1), pp. 31-38.
[9] R. Sarno, C. A. Djeni, I. Mukhlash and D. Sunaryono, Developing a Workflow Management System for Enterprise Resource Planning, (2015) *Journal of Theoretical and Applied Information Technology*, 72(3), pp. 412-421.
[10] R. Sarno, R. D. Dewandono, T. Ahmad, M. F. Naufal and F. Sinaga, Hybrid Association Rule Learning and Process Mining for Fraud Detection, (2015) *IAENG International Journal of Computer Science*, 42(2),pp. 59-72,.
[11] A. H. Basori, R. Sarno and S. Widyanto, The Development of 3D Multiplayer Mobile Racing Games Based On 3D Photo Satellite Map, (2008) *Proceedings of the IASTED International Conference on Wireless and Optical Communications*, pp. 1-5. http://dx.doi.org/10.1109/WOCN.2008.4542540
[12] R. Sarno, P. Sari, H. Ginardi dan D. Sunaryono, Decision Mining For Multi Choice Workflow Patterns, (2013) *Computer, Control, Informatics and Its Applications (IC3INA)*, pp. 337 - 342. http://dx.doi.org/ 10.1109/IC3INA.2013.6819197.
[13] Arcady A. Putilov, , Olga G. Donskaya, Construction and validation of the EEG analogues of the Karolinska sleepiness scale based on the Karolinska drowsiness test, (2013) *Clinical Neurophysiology*, 124(7), pp. 1346–1352. http://dx.doi.org/10.1016/j.clinph.2013.01.018.
[14] R. Nowak, Optimal Signal Estimation Using Cross-Validation, (1997) *Signal Processing Letters, IEEE*, 4 (1), pp. 23-25. http://dx.doi.org/10.1109/97.551692.
[15] M. Brass, M. Ullsperger, T. Knoesche, D. Cramon and N. Phillips, Who Comes First? The Role of the Prefrontal and Parietal Cortex in Cognitive Control, (2005) *Cognitive Neuroscience*, 17(9), pp. 1367 - 1375. http://dx.doi.org/10.1162/0898929054985400
[16] J. Fuster, The Prefrontal Cortex Makes the Brain a Preadaptive System, (2014) *Proceedings of the IEEE*, 102(4), pp. 417 - 426. http://dx.doi.org/10.1109/JPROC.2014.2306250
[17] S. Galetta, Occipital Lobe, (2014) *Encyclopedia of the Neurological Sciences (Second Edition)*, pp. 626–632. http://dx.doi.org/10.1016/B978-0-12-385157-4.01166-0.
[18] E. B. Johnson, E. M. Rees, I. Labuschagne, A. Durr, B. R. Leavitt, R. A. Roos, R. Reilmann, H. Johnson, N. Z. Hobbs, D. R. Langbehn, J. C. Stout, S. J. Tabrizi and R. I. Scahill, The impact of occipital lobe cortical thickness on cognitive task performance: An investigation in Huntington's Disease, (2015) *Neuropsychologia*, vol. 79, pp. 138–146. http://dx.doi.org/10.1016/j.neuropsychologia.2015.10.033
[19] O. Braddick, Occipital Lobe (Visual Cortex): Functional Aspects, (2015) *International Encyclopedia of the Social & Behavioral Sciences (Second Edition)*, pp. 127–132. http://dx.doi.org/10.1016/B978-0-08-097086-8.55041-7.

Authors' information

Riyanarto Sarno received M.Sc and Ph.D in Computer Science from the University of Brunswick Canada in 1988 and 1992.
His research includes Internet of Things, Enterprise Computing, Information Management, Intelligent Systems and Smart Grids.

Brilian T. Nugraha was born in Jambi, Indonesia. He is a fresh graduate of Informatics Department, Institut Teknologi Sepuluh Nopember, Surabaya, Indonesia. His major skills and researches are in Data/Signal Processing, Machine Learning, and Web Development.

Muhammad Nadzeri Munawar was born in Bandung, Indonesia. He is a fresh graduate of Informatics Department, Institut Teknologi Sepuluh Nopember, Surabaya, Indonesia. His major skills and researches are in Data/Signal Processing, Machine Learning, and Web Development.